Spin-orbit coupling and intrinsic spin mixing in quantum dots

C. F. Destefani,[1,2] Sergio E. Ulloa,[1] and G. E. Marques[2]
[1]*Department of Physics and Astronomy and Nanoscale and Quantum Phenomena Institute, Ohio University, Athens, Ohio 45701-2979, USA*
[2]*Departamento de Física, Universidade Federal de São Carlos, 13565-905 São Carlos, São Paulo, Brazil*
(Received 1 July 2003; revised manuscript received 17 November 2003; published 2 March 2004)

Spin-orbit coupling effects are studied in narrow-gap InSb quantum dots. Competition between different Rashba and Dresselhaus terms is shown to produce wholesale changes in the spectrum. The large (and negative) *g* factor and the Rashba field produce states where spin is no longer a good quantum number and intrinsic flips occur at moderate magnetic fields. For dots with two electrons, singlet-triplet mixing occurs in the ground state, with observable signatures in intraband far-infrared absorption, and possible importance in quantum computation.

DOI: 10.1103/PhysRevB.69.125302 PACS number(s): 73.21.La, 78.30.Fs, 71.70.Ej

I. INTRODUCTION

The creation and manipulation of spin populations in semiconductors has received a great deal of attention in recent years. Conceptual developments that have motivated these efforts include prominently the Datta-Das proposal for a spin field-effect transistor,[1] based on the Rashba spin-orbit coupling of electrons in a two-dimensional (2D) electron gas,[2] and the possibility of building quantum computation devices using quantum dots (QD's).[3] It is then important for full control of spin-flip mechanisms in nanostructures that all spin-orbit (SO) effects be understood.

There are two main SO contributions in zincblende materials: in addition to the structure inversion asymmetry (SIA) caused by the 2D confinement (the Rashba effect), there is a bulk inversion asymmetry (BIA) term in those structures (the Dresselhaus term).[4,5] Additional lateral confinement defining a QD introduces another SIA term with important consequences, as we will see in detail. Although the relative importance of these two effects depends on the materials and structure design (via interfacial fields), only recently have authors begun to consider the behavior of spins under the influence of all effects. For example, a modification of the Datta-Das design was recently suggested to allow for a diffusive version of the spin field-effect transistor,[6] and that proposal relies on the additional influence of the Dresselhaus SO coupling in the system.

In wide-gap materials (mainly GaAs) (Ref. 7) a unitary transformation has been used on the Hamiltonian of the system,[8] which yields an effective diagonal SO term incorporating the Rashba effect perturbatively. That approach is valid for GaAs due to its small SO coupling. However, in narrow-gap materials (such as InSb) where both SIA and BIA effects are anticipated to be much larger,[9] one requires the full Hamiltonian.

There are just a few works discussing SO effects in narrow-gap nanostructures. Among them, Ref. 10 uses a linear version of $\mathbf{k}\cdot\mathbf{p}$ theory in InSb QD's to include SIA terms from both the Rashba field *and* the lateral confinement which defines the QD. Only this last SIA term is considered in Ref. 13, and since it is diagonal in the Fock-Darwin (FD) basis no level mixing is found nor expected. In contrast, level mixing events are clearly identified in Ref. 10. Experiments in InSb QD's have explored the far-infrared (FIR) response in lithographically defined dots,[11] as well as photoluminescence features in self-assembled dots.[12]

The goal of this work is to show how important different types of SO couplings are in the spectra of parabolic QD's built in narrow-gap materials such as InSb. We consider the Rashba-SIA diagonal and SIA nondiagonal, as well as the Dresselhaus-BIA terms in the Hamiltonian, in order to study features of the spectrum as function of magnetic field, dot size, *g* factor, and electron-electron interaction. We draw attention to the appearance of strong level anticrossings (mixing) for moderate magnetic fields in typical QD's, and how this phenomenon is modified by the BIA terms not considered before.[10] As the level mixing involves states with different spin, strong *intrinsic* spin flips are found, *regardless* of the strength of the SO coupling, providing an important channel for spin decoherence in these systems. Moreover, measurement of FIR absorption would yield *direct* access to the coupling constants; i.e., the dispersion of FIR absorption peaks and appearance of additional split-off features are a direct consequence of the level mixing introduced by SO terms.

II. MODEL

Consider a heterojunction or quantum well confinement potential $V(z)$ such that only the lowest z subband is occupied. The Hamiltonian in the absence of SO interactions for a cylindrical QD is given by

$$H_0=\frac{\hbar^2}{2m}\mathbf{k}^2+V(\rho)+\frac{1}{2}g\mu_B\mathbf{B}\cdot\sigma, \tag{1}$$

where $\mathbf{k}=-i\boldsymbol{\nabla}+e\mathbf{A}/(\hbar c)$, and the vector potential $\mathbf{A}=B\rho(-\sin\theta,\cos\theta,0)/2$ describes a magnetic field $\mathbf{B}=B\mathbf{z}$; m is the effective mass in the conduction band,[16] g is the bulk g factor, μ_B is Bohr's magneton, $V(\rho)=\frac{1}{2}m\omega_0^2\rho^2$ is the lateral dot confinement with frequency ω_0, and σ is the Pauli spin vector. The analytical solution of H_0 yields the FD spectrum, $E_{nl\sigma_Z}=(2n+|l|+1)\hbar\Omega+l\hbar\omega_C/2+g\mu_B B\sigma_Z/2$, with effective (cyclotron) frequency given by $\Omega=\sqrt{\omega_0^2+\omega_C^2/4}\,[\omega_C$

TABLE I. All of the terms present in the expression for the cubic Dresselhaus SO contribution.

Term	$i=1$	$i=2$	$i=3$	$i=4$
A_{i1}	$-\frac{1}{4}$	$-\frac{1}{4}$	$\frac{1}{4}$	$\frac{1}{4}$
A_{i2}	$\frac{3}{4}(1+L_z)$	$\frac{3}{4}(1-L_z)$	$\frac{1}{4}(1+L_z)$	$\frac{1}{4}(1-L_z)$
A_{i3}	$-\frac{3}{4}(1+3L_z+L_z^2)$	$-\frac{3}{4}(1-3L_z+L_z^2)$	$-\frac{1}{4}(1-L_z+L_z^2)$	$-\frac{1}{4}(1+L_z+L_z^2)$
A_{i4}	$\frac{1}{4}(8L_z+6L_z^2+L_z^3)$	$\frac{1}{4}(-8L_z+6L_z^2-L_z^3)$	$\frac{1}{4}(2L_z^2-L_z^3)$	$\frac{1}{4}(2L_z^2+L_z^3)$
B_{i1}	$\frac{3}{8}$	$-\frac{3}{8}$	$\frac{1}{8}$	$-\frac{1}{8}$
B_{i2}	$-\frac{3}{8}(1+2L_z)$	$-\frac{3}{8}(-1+2L_z)$	$-\frac{1}{8}(5+2L_z)$	$-\frac{1}{8}(-5+2L_z)$
B_{i3}	$\frac{3}{8}(2L_z+L_z^2)$	$\frac{3}{8}(2L_z-L_z^2)$	$-\frac{3}{8}(2L_z+L_z^2)$	$-\frac{3}{8}(2L_z-L_z^2)$
C_{i1}	$-\frac{3}{16}$	$-\frac{3}{16}$	$-\frac{1}{16}$	$-\frac{1}{16}$
C_{i2}	$\frac{3}{16}L_z$	$-\frac{3}{16}L_z$	$-\frac{1}{16}(8+3L_z)$	$-\frac{1}{16}(8-3L_z)$
D_{i1}	$\frac{1}{32}$	$-\frac{1}{32}$	$-\frac{1}{32}$	$\frac{1}{32}$

$=eB/(mc)$]. The FD states are given in terms of Laguerre polynomials.[17] The confinement, magnetic, and effective lengths are $l_0=\sqrt{\hbar/(m\omega_0)}$, $l_B=\sqrt{\hbar/(m\omega_C)}$, and $\lambda=\sqrt{\hbar/(m\Omega)}$, respectively.

The SIA term[2] for the full confining potential, $V(\mathbf{r})=V(\rho)+V(z)$, and coupling parameter α is given by $H_{SIA}=\alpha\boldsymbol{\sigma}\cdot(\boldsymbol{\nabla}V\times\mathbf{k})$; it can be decomposed, in cylindrical coordinates, as $H_{SIA}=H_R+H_{SIA}^D+H_K$, where $H_K=i\alpha(\hbar\omega_0/l_0^2)\lambda x(\sigma_+L_--\sigma_-L_+)\langle k_z\rangle$ is zero because $\langle k_z\rangle=0$,

$$H_{SIA}^D=\alpha\frac{\hbar\omega_0}{l_0^2}\sigma_Z\left(L_Z+\frac{\lambda^2}{l_B^2}\frac{x^2}{2}\right) \tag{2}$$

is the diagonal contribution due to the lateral confinement, and

$$H_R=-\alpha\frac{dV}{\lambda dz}[\sigma_+L_-A_-+\sigma_-L_+A_+] \tag{3}$$

is the Rashba term associated with the perpendicular confinement field, dV/dz. In the last equations, $L_\pm=e^{\pm i\theta}$, $\sigma_\pm=(\sigma_X\pm i\sigma_Y)/2$, $x=\rho/\lambda$ is an adimensional radial coordinate, $L_Z=-i\partial/\partial\theta$ is the z-orbital angular momentum, and $A_\pm=\mp\partial/\partial x+L_Z/x+x\lambda^2/(2l_B^2)$. Notice that both terms are, in principle, tunable; H_{SIA}^D depends on the confining frequency ω_0, while H_R depends on the interfacial field dV/dz.

In zincblende materials one should also consider the BIA Hamiltonian[4] given by $H_{BIA}=\gamma[\sigma_xk_x(k_y^2-k_z^2)+\sigma_yk_y(k_z^2-k_x^2)+\sigma_zk_z(k_x^2-k_y^2)]$, where γ is the coupling parameter. After averaging along the z direction of quantization, one obtains $H_{BIA}=\gamma[\sigma_xk_xk_y^2-\sigma_yk_yk_x^2]+\gamma\langle k_z^2\rangle[\sigma_yk_y-\sigma_xk_x]+\gamma\sigma_z\langle k_z\rangle(k_x^2-k_y^2)$, where the first (second) term is cubic (linear) in the in-plane momentum, and the last term is zero because $\langle k_z\rangle=0$, while $\langle k_z^2\rangle\simeq(\pi/z_0)^2$, z_0 being the z-direction confinement length. One can decompose it in cylindrical coordinates as $H_{BIA}=H_D^L+H_D^C$, where the linear Dresselhaus contribution is given by

$$H_D^L=i\frac{\gamma\langle k_z^2\rangle}{\lambda}[\sigma_+L_+A_+-\sigma_-L_-A_-], \tag{4}$$

and the cubic term can be expressed, after some algebra,[18] as

$$\begin{aligned}H_D^C=i\frac{\gamma}{\lambda^3}\Bigg\{&\sigma_-L_+^3\left[A_1+\frac{\lambda^2}{l_B^2}B_1+\frac{\lambda^4}{l_B^4}C_1+\frac{\lambda^6}{l_B^6}D_1\right]\\&+\sigma_+L_-^3\left[A_2+\frac{\lambda^2}{l_B^2}B_2+\frac{\lambda^4}{l_B^4}C_2+\frac{\lambda^6}{l_B^6}D_2\right]\\&+\sigma_-L_-\left[A_3+\frac{\lambda^2}{l_B^2}B_3+\frac{\lambda^4}{l_B^4}C_3+\frac{\lambda^6}{l_B^6}D_3\right]\\&+\sigma_+L_+\left[A_4+\frac{\lambda^2}{l_B^2}B_4+\frac{\lambda^4}{l_B^4}C_4+\frac{\lambda^6}{l_B^6}D_4\right]\Bigg\},\end{aligned} \tag{5}$$

where we define the operators $A_i=A_{i1}(\partial^3/\partial x^3)+A_{i2}(1/x)(\partial^2/\partial x^2)+A_{i3}(1/x^2)(\partial/\partial x)+A_{i4}(1/x^3)$, $B_i=B_{i1}x(\partial^2/\partial x^2)+B_{i2}(\partial/\partial x)+B_{i3}(1/x)$, $C_i=C_{i1}x^2(\partial/\partial x)+C_{i2}x$, and $D_i=D_{i1}x^3$, with $i=1,2,3,4$; each one of the terms compacted in these operators is explicitly given in Table I. Notice that at finite magnetic field, the matrix elements with $\sigma_\pm L_\pm$ in H_D^C are not Hermitian, requiring the usual symmetrization;[8] at zero field, this problem does not occur.[14]

For the electron-electron interaction $H_{ee}=e^2/(\varepsilon|\mathbf{r}_1-\mathbf{r}_2|)$, with ε being the dielectric constant of the material, we use an expansion in Bessel functions J_k for the term $|\mathbf{r}_1-\mathbf{r}_2|^{-1}$; with an adimensional parameter ξ, the interaction can be expressed as

$$H_{ee}=\frac{\hbar\Omega\lambda}{a_B}\sum_{k=-\infty}^{\infty}e^{ik(\theta_1-\theta_2)}\int_0^\infty d\xi J_k(\xi x_1)J_k(\xi x_2)e^{-\xi z_0/\lambda}, \tag{6}$$

where $a_B=\varepsilon\hbar^2/(me^2)$ is the effective Bohr radius of the system. The FD basis states are properly antisymmetrized, describing the unperturbed spin eigenstates.[18]

From these expressions, it is clear that the total single-particle Hamiltonian is given by $H=H_0+H_{SIA}+H_{BIA}=H_0+H_{SIA}^D+H_R+H_D^L+H_D^C$; when dealing with the two-particle case, we must add H_{ee} to H.

The general forms of the various SO terms in the single-particle Hamiltonian exhibit interesting characteristics: (i) The magnetic field plays an important role via its linear de-

pendence in H_{SIA}^D, H_R, and H_D^L, or its linear to cubic dependence in H_D^C. (ii) The Hamiltonian yields selection rules explicitly, dictating which levels $\{n,l,\sigma_Z\}$ will be influenced by the SO effects. (iii) At zero field and due to the $\sigma_Z L_Z$ term, H_{SIA}^D splits the spectrum according to the total z-angular momentum $j=l+\sigma_Z/2$. (iv) At finite field, H_R induces a set of anticrossings in the FD spectrum whenever $\Delta l=\pm 1=-\Delta\sigma_Z/2$; due to the $\sigma_\pm L_\mp$ terms, mostly negative l's are affected since their magnetic dispersions allow for crossings; the lowest anticrossing occurs between the levels $\{0,0,-1\}$ and $\{0,-1,+1\}$. (v) The H_D^C term, via $\sigma_\mp L_\pm^3$ terms, induces a set of anticrossings in levels where $\Delta l=\mp 3$ and $\Delta\sigma_Z/2=\pm 1$; the first one at low field involves the levels $\{0,1,-1\}$ and $\{0,-2,+1\}$. (vi) The terms $\sigma_\pm L_\pm$ in H_D^L and H_D^C do not induce anticrossings, but split and shift the FD spectrum due to matrix elements where $\Delta l=\pm 1=\Delta\sigma_Z/2$. Notice that matrix elements between states with different n's are in general nonzero, so that the full diagonalization involves mixings with various n values.

Regarding H_{ee}, the Coulomb interaction is able to split the spectrum at zero field into singlet and triplet sets. A magnetic field may affect the sequence of levels; for example, the QD ground state may oscillate between singlet and triplet as the field is increased.

III. RESULTS

We present results by discussing the role of the different SO terms in the Hamiltonian. We have isolated each contribution and present here the summary of our findings. The sequence of FD states of H_0 starts at zero B field with $\{n,l,\sigma_Z\}=\{0,0,\pm 1\}$, followed by the degenerate set of $\{0,-1,\pm 1\}$ and $\{0,1,\pm 1\}$.[17] Spin and orbital degeneracies are broken by B and the states with negative l and positive σ_Z acquire lower energies because of the *negative g* factor. The lowest FD energy level crossing is between states $\{0,0,-1\}$ and $\{0,-1,+1\}$, and occurs at

$$B_C^0=\frac{\hbar\omega_0}{\mu_B}\frac{\tilde{m}}{\sqrt{\tilde{m}|g|(\tilde{m}|g|+2)}}, \tag{7}$$

where $\tilde{m}=m/m_0$. The moderate value of B_C^0 in InSb is a direct consequence of its large $|g|$ factor.[15] For GaAs ($|g|=0.44$, $\tilde{m}=0.067$), this level crossing appears only at $B_C^{0(GaAs)}\simeq 9.5$ T for a much smaller confinement, $\hbar\omega_0=2$ meV, and in the regime where Landau levels are well defined. Weaker confinement (smaller ω_0) shifts this crossing to lower fields. Notice that for $g<0$, H_R mixes these states and H_D^L shifts the crossing to higher fields. In materials with $g>0$, the role of these two terms would be interchanged: H_D^L would produce relatively stronger level anticrossings, while H_R would only shift the spectrum weakly. So, in nonzincblende materials such as silicon, H_D^L is absent and no anticrossing occurs.

The energy spectrum for the full single-particle H in InSb QD's (Ref. 15) is presented in Fig. 1(a) vs B field. It is obtained by direct diagonalization using a FD basis with $n\leqslant 4$ (or ten energy ''shells''), i.e., 110 basis states. Let us discuss the progressive changes to the FD levels induced by the separated addition of each one of the SO terms in H.

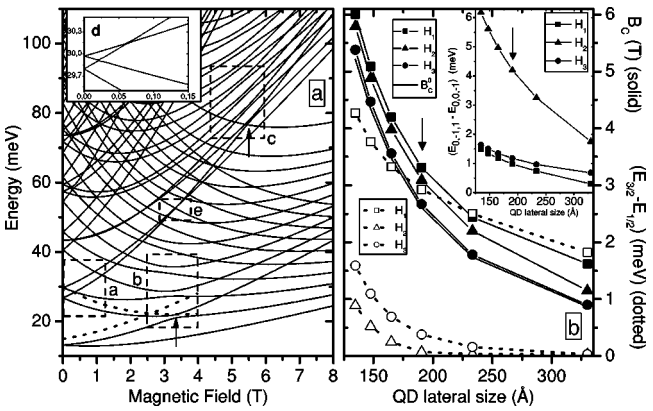

FIG. 1. (a) Single-particle spectrum for full Hamiltonian H vs B field for an InSb QD as in Ref. 15. Highlights in dashed boxes: a shows zero-field splitting in second shell (affected mostly by BIA terms), and crossing at $B\simeq 0.3$ T. Compare with inset d with only SIA terms and *two* crossings at 0.02 and 0.06 T, and much smaller zero-field splitting (box displaced for clarity). Second crossing for this shell in full H is at $B\simeq 3.4$ T (e box). Boxes b and c indicate anticrossings (AC's) induced by Rashba term H_R with $\Delta l=-\Delta\sigma_Z/2=\pm 1$; first AC indicated by arrow in b (c) involves states $\{0,0,-1\}$ and $\{0,-1,+1\}$ ($\{0,1,-1\}$ and $\{1,0,+1\}$). Dotted lines at low energy show FD level crossing at $B_C^0\simeq 2.6$ T. (b). Dependence on lateral dot size l_0. Dotted lines: SO zero-field splitting in a box on left panel. Solid lines: B_C field of first AC in b box on left panel; inset shows energy splitting at that AC. Arrows at $l_0=190$ Å show QD size for spectrum in (a). H_1 curves (squares) use Ref. 15, H_2 (triangles), and H_3 (circles) use same parameters but four times stronger Rashba field (H_2) or twice as large z_0 (H_3). Both latter cases increase relative strength of SIA terms. Solid line with no symbol shows B_C^0 in Eq. (7).

The addition of the diagonal H_{SIA}^D term to H_0 shifts energies and causes a small zero-field splitting in the spectrum, but does not change appreciably the position of the first crossing, Eq. (7), shown by the dotted lines in Fig. 1(a) at $B_C^0\simeq 2.6$ T. The shifts induce two new crossings at low fields (inset d), since the SO orders states according to their j value, and the highest (lowest) state at zero field has $j=3/2$ (1/2) in the second shell. At $B\simeq 0.2$ T one recovers the ''normal'' sequence of states in this shell for $g<0$: $\{0,-1,+1\}$, $\{0,-1,-1\}$, $\{0,1,+1\}$, $\{0,1,-1\}$. Such competition between SO and magnetic field is similar to the Zeeman and Paschen-Back regimes in atoms.[19] This level ordering is also observed in Ref. 13.

The addition of the nondiagonal Rashba contribution H_R to H_0 introduces strong state mixing for *any* value of α, whenever FD levels with $\Delta l=-\Delta\sigma_Z/2=\pm 1$ cross. This mixing converts the crossings at B_C^0 to clear anticrossings or ''minigaps.'' Higher levels satisfying these selection rules also display anticrossings at nearly the same field. The field width and minigaps are determined by the value of α, while B_C, where the anticrossing occurs, is nearly insensitive to α.

The addition of the cubic Dresselhaus term H_D^C to H_0

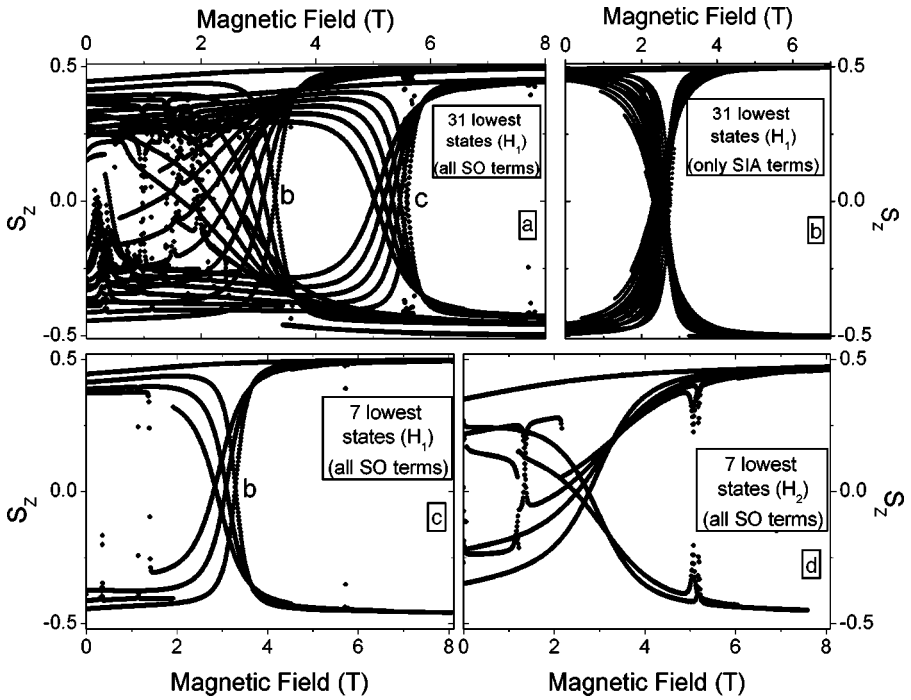

FIG. 2. (a) S_Z vs B field for lowest 31 states of full single-particle H; b and c labels refer to minigaps in boxes in Fig. 1(a). Higher energy anticrossings in each set are shifted to lower fields. If only H_{SIA} terms are considered (b), all spin mixing occurs at field $B_C \simeq B_C^0 \simeq 2.6$ T. (c) S_Z for lowest seven states of full single-particle H; complete spin mixing at anticrossing is obvious. (d) Dot with Rashba field four times stronger, where a mixing at $B \simeq 1.2$ T as caused by H_D^C and involving the states $\{0,1,-1\}$ and $\{0,-2,+1\}$ becomes visible. Increasing H_R produces stronger spin mixing (H_1 and H_2 labels defined as in Fig. 1).

induces anticrossings (via $\sigma_{\mp} L_{\pm}^3$) and zero-field splittings (via $\sigma_{\pm} L_{\pm}$) in the FD spectrum. The splittings are much smaller than those induced by H_R and practically unnoticeable in the spectrum, reflecting the smallness of E_D^C.[15] Its influence, as we will see, will be stronger if the Rashba field dV/dz is increased.

The addition of the linear H_D^L contribution to H_0, however, has a much bigger impact on the zero-field splittings, which can in principle be tuned by changing the effective well size z_0. H_D^L alone induces such a strong mixing at low fields that one cannot identify different Zeeman and Paschen-Back regimes.

Let us now comment on the features of the full single-particle spectrum of H [Fig. 1(a)]. A first group of minigaps (for $n=0$ levels) is induced by H_R (and shifted to higher field by H_D^L), so that $B_C^0 \rightarrow B_C \simeq 3.3$ T (box b and lower arrow). The group in box c at $B \simeq 5.5$ T (first anticrossing is indicated by an arrow) is also due to H_R and arises from the $n=1$ level manifold. The single crossing in box a in the second shell at $B \simeq 0.3$ T is dominated by H_D^L, the same as the crossing in box e (compare with inset d for a truncated Hamiltonian with only $H_0 + H_{SIA}$, with two low-field crossings). The sequence of the first excited levels at zero field is $j=3/2$ (1/2) for the highest (lowest) state, while at higher energies both SIA and BIA terms cooperate to produce anticrossings [not visible at the resolution in Fig. 1(a)].

One can further appreciate the intricate balance of SO terms by analyzing how various quantities are affected by changes in the lateral and vertical sizes, l_0 and z_0, or Rashba field dV/dz, as shown on Fig. 1(b). The zero-field splitting (dotted lines) is dominated by the linear BIA contribution for any value of l_0 here. Increasing z_0 strongly reduces the splittings because the Dresselhaus contribution weakens (H_3, $\bigcirc$ symbols). The reduction is more drastic if one increases dV/dz (H_2, $\triangle$ symbols), which makes H_R bigger and can then cancel or suppress the zero-field splitting produced by H_{BIA} (label H_1 refers to Ref. 15). By working with only H_R and H_D^L terms, authors have mentioned the possibility of tuning SO terms to obtain total cancellation of the zero-field splitting.[6] However, H_{SIA}^D and H_D^C are also important for this cancellation, shifting down the needed values of z_0 or Rashba field by 10%. We observe that even if one may eliminate the zero-field splitting, such tuning has nearly no effect on the anticrossing at finite field. Measurement of both quantities on the same sample should yield important information on the relative strength of parameters α and γ. This would contribute to better define their values from the rather broad range reported in the literature.[15]

The anticrossing field B_C [solid lines in Fig. 1(b)] decreases with QD size, as expected from Eq. (7), $B_C^0 \simeq \omega_0 \simeq 1/\sqrt{l_0}$. A finite α slightly increases B_C, but the BIA contribution increases it considerably. Increasing z_0 or dV/dz decreases B_C, since this decreases H_{BIA}. One can estimate that at $l_0 = 270$ Å ($\hbar\omega_0 = 7.5$ meV), $B_C \simeq 2.1$ T, while it shifts to 1.8 T if dV/dz is four times larger (H_2 label). If z_0 is doubled (H_3 label), B_C shifts to 1.5 T. We can use this last value to make a comparison with Ref. 10, where BIA terms are absent and $B_C \simeq 1.7$ T; the small (0.2 T) difference can be attributed to nonparabolicity effects there taken into account.[16] Anticrossings at such low fields may be interesting for applications due to easier access.

The minigaps at $B_C \simeq 3.3$ T [inset in Fig. 1(b)] have their main origin from the H_R term. Inclusion of H_{BIA} reduces the splitting substantially. If z_0 is changed from 40 to 80 Å (H_3 label) the splitting is enhanced slightly, but larger z_0 produces no significant changes. However, the splitting can be drastically enhanced by increasing the Rashba field; for example, it changes from 1 to 4.2 meV at $l_0 = 190$ Å if the interfacial field is increased fourfold (H_2 label).

Figure 2 illustrates the importance of the level anticross-

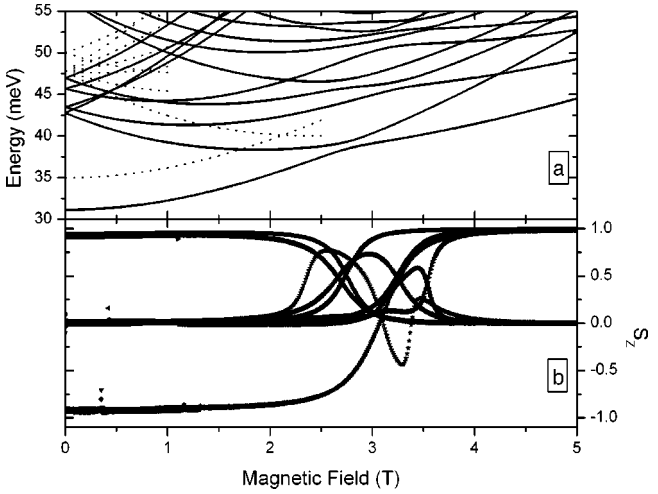

FIG. 3. (a) Two-particle QD energy spectrum vs B field (basis included 190 states, only lowest levels shown). Solid (dotted) lines refer to $H+H_{ee}$ (H_0+H_{ee}). With no SO (dotted lines) and at $B=0$, ground state is a singlet ($\{L_Z,S_Z\}=\{0,0\}$) at 35 meV; the first (second) excited state is a triplet (singlet) $\{\pm 1,\pm 1\}$ and $\{\pm 1,0\}$ ($\{\pm 1,0\}$) at 48 meV (50 meV). Notice that SO coupling and H_{ee} have opposite effects and levels are shifted back to energies close to the noninteracting case when SO is taken into account. Lowest anticrossing at $B\simeq 2.7$ T is between $\{0,0\}$ and $\{-1,1\}$ states, induced by H_R (label L_Z refers to the two-particle z-orbital angular momentum). (b) S_Z for nine lowest states of the two-particle QD.

ings on the spin, as the expectation value of $S_Z=\sigma_Z/2$ for each state is plotted vs B. Figures 2(a) and 2(b) include all states with $E\lesssim 80$ meV (for full SO and only SIA terms, respectively), while Figs. 2(c) and 2(d) focus only on the lowest seven levels of the full single-particle Hamiltonian. Although a large majority of states have S_Z close to $\pm 1/2$, as one expects for pure states, there are significant deviations. The various SO terms mix levels close to accidental degeneracy points in the FD spectrum and produce the large deviations seen here. Figure 2(a) shows B_C values where states in the boxes b and c of Fig. 1(a) reverse their spins. Figure 2(c) shows how H_R produces an *intrinsic* (i.e., no phonon-assisted) total collapse of the spin number for the low energy states in the QD;[20] although the ground state is nearly pure ($S_Z\simeq 1/2$, and more so at higher B), the first few excited states totally mix at $B_C\simeq 3.3$ T [compare with Fig. 2(b) where only SIA terms are taken into account and *all* QD levels, except the ground state, collapse at $B_C\simeq B_C^0=2.6$ T]. Figure 2(d) shows how a stronger Rashba field ($dV/dz=-2\times 10^{-3}$ eV/Å) greatly widens the mixing region and lowers the field to $B_C\simeq 2.8$ T; most importantly, it makes visible the anticrossing due to the cubic Dresselhaus term at $B\simeq 1.2$ T, involving the states $\{0,1,-1\}$ and $\{0,-2,+1\}$.

Figure 3(a) shows the lowest energy states for a two-electron QD. Dotted lines show energy dispersions for H_0+H_{ee} (no SO terms); by comparing with a noninteracting two-electron QD, notice that the direct Coulomb interaction increases ($\simeq 5$ meV) the singlet ground-state energy, whereas the exchange term creates a new zero-field splitting ($\simeq 2$ meV) between first (triplet) and second (singlet) excited states. Solid lines show energy dispersions for $H+H_{ee}$ (full two-electron Hamiltonian); notice mainly that: (i) SO coupling and H_{ee} have opposite effects on the spectrum; (ii) the SO coupling lifts the degeneracies of singlet and triplet excited states and defines new zero-field splittings; (iii) the minigap at $B_C\simeq 3.3$ T of Fig. 1(a) occurs here at $B\simeq 2.7$ T and it is related to a singlet-triplet mixture *now involving* the QD ground state. Figure 3(b) shows the S_Z dependence (do not confuse with S_Z for the single-particle case of Fig. 2) on B for $H+H_{ee}$ states; observe the strong intrinsic spin mixing around 2.7 T. Due to this mixing, a singlet-triplet transition (qubit) involving the QD ground state becomes possible and, in principle, may be explored in implementations of quantum computing devices. Moreover, the splitting will also be apparent in the FIR response of QD's, allowing the determination of the various SO coupling strengths.

IV. CONCLUSIONS

We have shown that inclusion of all SO terms is essential in order to obtain a complete picture of the level structure in narrow-gap QD's, and have discussed the role played by each one of the Rashba and Dresselhaus terms in QD's spectrum. The combination of strong SO coupling in H_R and large (and negative) g factor introduces strong intrinsic mixing of the low excitations for the single-particle spectrum; the magnetic field where such mixing occurs is shifted by H_D^L to higher fields. Correspondingly, the two-particle spectrum exhibits strong singlet-triplet coupling at moderate fields, with significant experimental consequences like possible use in qubits design. Observation of FIR mode magnetic dispersion would allow the direct determination of coupling constants.

ACKNOWLEDGMENTS

We acknowledge support from FAPESP-Brazil, US DOE Grant No. DE-FG02-91ER45334, and the CMSS Program at OU.

[1] S. Datta, and B. Das, Appl. Phys. Lett. **56**, 665 (1990).
[2] Y.A. Bychkov, and E.I. Rashba, J. Phys. C **17**, 6039 (1984).
[3] D. Loss, and D.P. DiVincenzo, Phys. Rev. A **57**, 120 (1998); X. Hu, and S. Das Sarma, *ibid.* **64**, 042312 (2001).
[4] G. Dresselhaus, Phys. Rev. **100**, 580 (1955).
[5] One should also mention the recently discovered microscopic SIA that occurs in heterojunctions and produces hole band mixings and strong optical-absorption anisotropy [O. Krebs and P. Voison, Phys. Rev. Lett. **77**, 1829 (1996)]; see especially U. Rössler and J. Kainz, Solid State Commun. **121**, 313 (2002), for a dis-

cussion of the spin splittings in the electron subbands.

[6] J. Schliemann, J.C. Egues, and D. Loss, Phys. Rev. Lett. **90**, 146801 (2003).

[7] J.B. Miller, D.M. Zumbühl, C.M. Marcus, Y.B. Lyanda-Geller, D. Goldhaber-Gordon, K. Campman, and A.C. Gossard, Phys. Rev. Lett. **90**, 076807 (2003); M. Valín-Rodríguez, A. Puente, Llorenç Serra, and E. Lipparini, Phys. Rev. B **66**, 235322 (2002).

[8] A.V. Khaestkii and Y.V. Nazarov, Phys. Rev. B **64**, 125316 (2001); I.L. Aleiner and V.I. Fal'ko, Phys. Rev. Lett. **87**, 256801 (2001); L.M. Woods, T.L. Reinecke, and Y. Lyanda-Geller, Phys. Rev. B **66**, 161318 (2002).

[9] M. Cardona, N.E. Christensen, and G. Fasol, Phys. Rev. B **38**, 1806 (1988).

[10] T. Darnhofer, and U. Rössler, Phys. Rev. B **47**, 16 020 (1993).

[11] P. Junker, U. Kops, U. Merkt, T. Darnhofer, and U. Rössler, Phys. Rev. B **49**, 4794 (1994).

[12] E. Alphandéry, R.J. Nicholas, N.J. Mason, S.G. Lyapin, and P.C. Klipstein, Phys. Rev. B **65**, 115322 (2002).

[13] O. Voskoboynikov, C.P. Lee, and O. Tretyak, Phys. Rev. B **63**, 165306 (2001).

[14] S. Gopalan, J.K. Furdyna, and S. Rodriguez, Phys. Rev. B **32**, 903 (1985).

[15] The material parameters we use for InSb are $m=0.014m_0$, $g=-51$, $\varepsilon=16.5$, $a_B=625$ Å, $\alpha=500$ Å^2, and $\gamma=160$ eV Å^3, while for typical dot characteristics we use $\hbar\omega_0=15$ meV ($l_0=190$ Å), $z_0=40$ Å, and Rashba field $dV/dz=-0.5\times10^{-3}$ eV/Å, if no other numbers are specified. These values yield *prefactors* at zero B field of $E_{SIA}^D=\alpha\hbar\omega_0/l_0^2=0.2$, $E_R=-(\alpha/\lambda)dV/dz=1.3$, $E_D^C=\gamma/\lambda^3=0.02$, $E_D^L=\gamma\langle k_z^2\rangle/\lambda=5.2$, and $E_{ee}=\hbar\Omega\lambda/a_B=4.5$, all in meV; this illustrates the order of magnitude of the various terms, although the contributions will be different for different levels and change with model parameters and magnetic field. Other (larger) values of γ appear in the literature, and we use this to avoid overestimating its role in the spectrum.

[16] Nonparabolicity is important in InSb but its effect is ignored here, as it does not introduce spin mixing. Its main effect is to shift energy levels somewhat, which will in turn shift the critical field B_C.

[17] L. Jacak, A. Wojs, and P. Hawrylak, *Quantum Dots* (Springer, Berlin, 1998).

[18] C.F. Destefani, Ph.D. dissertation, Universidade Federal de São Carlos, Brazil, 2003.

[19] J.J. Sakurai, *Modern Quantum Mechanics* (Addison-Wesley, Reading, 1994).

[20] The appearance of minigaps Δ in the spectrum would produce strong spin flips with a rate $\Gamma\simeq\hbar/\Delta$. Notice, of course, that the strong spin mixing yields intrinsically impure states.